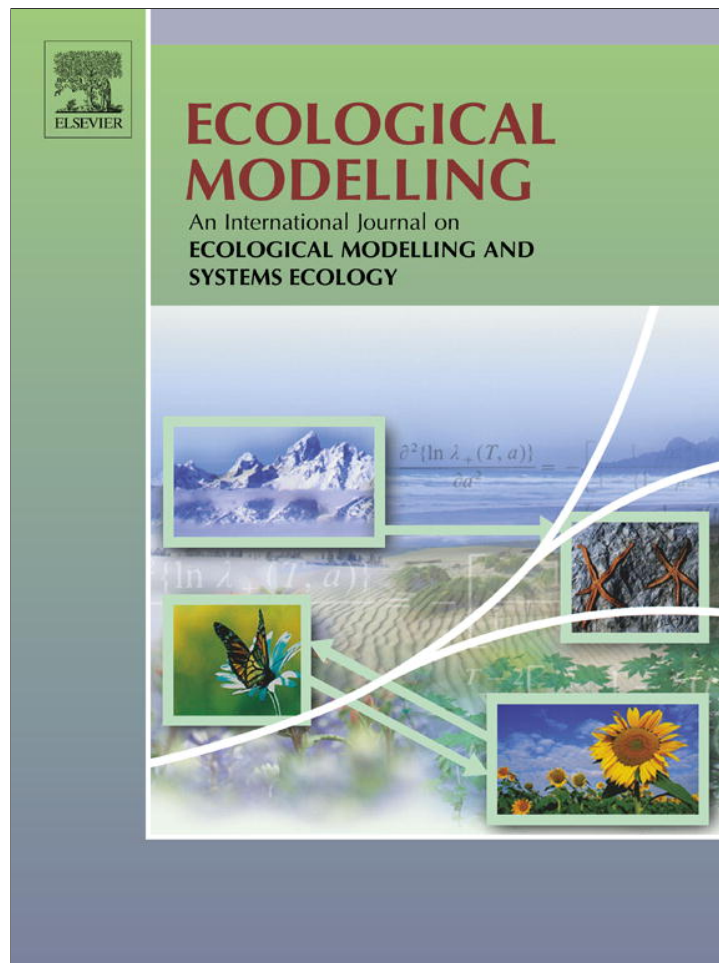


Provided for non-commercial research and education use.
Not for reproduction, distribution or commercial use.



(This is a sample cover image for this issue. The actual cover is not yet available at this time.)

This article appeared in a journal published by Elsevier. The attached copy is furnished to the author for internal non-commercial research and education use, including for instruction at the authors institution and sharing with colleagues.

Other uses, including reproduction and distribution, or selling or licensing copies, or posting to personal, institutional or third party websites are prohibited.

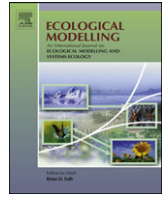
In most cases authors are permitted to post their version of the article (e.g. in Word or Tex form) to their personal website or institutional repository. Authors requiring further information regarding Elsevier's archiving and manuscript policies are encouraged to visit:

<http://www.elsevier.com/copyright>



Contents lists available at SciVerse ScienceDirect

Ecological Modelling

journal homepage: www.elsevier.com/locate/ecolmodel

What mark variograms tell about spatial plant interactions

Arne Pommerening^{a,*}, Aila Särkkä^{b,c,1}^a Bern University of Applied Sciences, School of Agricultural, Forest and Food Sciences HAFL, Länggasse 85, CH-3052 Zollikofen, Switzerland^b Department of Mathematical Sciences, Chalmers University of Technology, 412 96 Gothenburg, Sweden^c Department of Mathematical Sciences, University of Gothenburg, 412 96 Gothenburg, Sweden

ARTICLE INFO

Article history:

Received 11 September 2012

Received in revised form

30 November 2012

Accepted 3 December 2012

Keywords:

Plant interactions

Negative autocorrelation

Individual-based model

Evolution of spatial tree patterns

Plant interactions

Disturbances

ABSTRACT

Many if not all data collected in ecology have both a spatial as well as a temporal dimension. This suggests the use of summary characteristics from spatial statistics to gain more refined insight into plant interactions. Spatial tree data can for example be considered as point patterns (formed by tree locations) with attached marks (e.g. tree sizes). If only the pattern of tree locations is of interest one can use for example the pair correlation function. If in addition, the sizes (or some other characteristics) of trees or other plants are of interest, marked summary statistics can be more suitable. In this paper, we propose the so-called mark variogram as a useful tool in ecological studies. This summary characteristic basically indicates how similar two plants within a certain distance from each other are. For example, if two plants are approximately of the same size, the mark variogram has small values, and if their sizes differ somewhat, the mark variogram has large values. Recently, there has been a lot of discussion on how to interpret the shape of mark variograms caused by pairs of plants with different sizes at close proximity. Such variogram shapes exhibiting so-called negative autocorrelation, another expression for high small-scaled size diversity, are assumed to indicate strong competition between plants.

In this study, we reconstructed two spatial tree time series where negative autocorrelation has occurred and also simulated four alternative forest development paths in order to experimentally explore the causes of negative autocorrelation.

Interestingly the results highlighted that man-made disturbances (e.g. thinnings) often result in a significant number of pairs of large and small trees at close proximity leading to negative autocorrelation. We could also show that whilst negative autocorrelation can be the consequence of natural forest development including competition processes, it can, however, also be the consequence of disturbances and of subsequent colonisation by small trees.

Since disturbances play an important role in the development of negative autocorrelation, the mark variogram is a key summary characteristic in disturbance ecology.

© 2012 Elsevier B.V. All rights reserved.

1. Introduction

The spatial pattern of plants can be considered a realisation of a spatial marked point process. The locations of the plants are the points and some characteristic of the plants (e.g. diameter) is the mark. The mark variogram is a summary characteristic that can be used to identify the influence of interactions between plants as well as of environmental factors on size characteristics of plants (Cressie, 1993; Illian et al., 2008; see also Section 2.2 for statistical details).

During the last 20 years the mark variogram has been successfully used as a statistical tool in plant ecology and forestry. Biondi

et al. (1994) for example studied growth processes in old-growth ponderosa pine forests in Arizona. In their analysis the points are tree locations and the marks are 10-year basal area increments. The corresponding empirical mark variograms of some of the research plots had the shape of variograms with *negative autocorrelation* where the empirical mark variogram decreased with increasing distance r for small r (black curve in Fig. 1). For larger r , the empirical mark variogram increased and took the form of a geostatistical variogram, which typically increases with increasing r . Biondi et al. (1994) ignored the behaviour of the empirical mark variogram for small r and approximated it by a typical geostatistical variogram, with the aim of providing information on the long-range variability of basal area increments. Wälder and Stoyan (1996) and Stoyan and Wälder (2000) used the same data and discussed the unusual shape of the mark variogram by concentrating on short distances. They concluded that the shape was caused by a high frequency of pairs of dominant and suppressed trees at close proximity. In the studied data the occurrence of dominant and suppressed trees is

* Corresponding author. Tel.: +41 031 910 22 76; fax: +41 031 910 22 99.
E-mail addresses: arne.pommerening@bfh.ch, arne.pommerening@gmail.com (A. Pommerening), aila@chalmers.se (A. Särkkä).

¹ Tel.: +46 031 772 35 42; fax: +46 031 772 35 08.

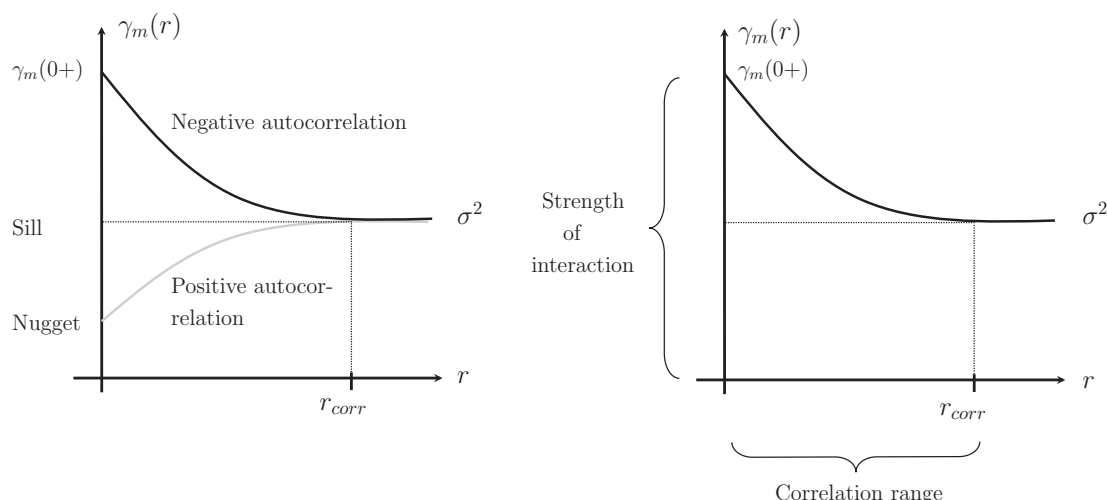


Fig. 1. The form of a mark variogram, $\gamma_m(r)$, influenced by interaction between plants (negative autocorrelation variograms, black curve) compared to the standard form of a geostatistical variogram, $\gamma_m(r)$ (grey). r is the interpoint distance, r_{corr} the correlation range and σ^2 the field variance or variance of marks (also referred to as sill). Nugget is related to the inherent variability in the investigated pattern at very small scale.

a significant property of the woodland community and therefore should not be ignored.

Kint et al. (2003) analysed tree heights in mixed Scots pine (*Pinus sylvestris* L.) forests in Belgium with mark variograms and also found variogram shapes reflecting negative autocorrelation. The authors attributed these shapes to spatial interaction between trees at short distances.

Dimov et al. (2005) in another study analysed the spatial continuity of tree basal area and crown projection area of four mixed hardwood forests in Louisiana, Arkansas and Mississippi with mark variograms. They also identified mark variograms with negative autocorrelation at short distances. In an attempt to investigate the long-range behaviour of trees they manipulated the data and excluded suppressed trees from the analysis to obtain variograms reflecting only positive autocorrelation.

Suzuki et al. (2008) analysed the spatio-temporal pattern of a mixed *Abies* forest in Japan. The authors used mark variogram, pair correlation function, and mark correlation function with tree heights as marks for six spatial surveys over a total time period of 47 years following a large disturbance in 1959. During this period no human interventions took place other than the occasional removal of wind-thrown trees. This study is particularly remarkable since it is one of the few cases that show the gradual evolution of a negative autocorrelation variogram over time. The authors concluded that the variogram shape developed as a result of high mortality in clusters of suppressed trees, which increased the probability of pairs of different sized trees at close proximity.

In particular, the last study suggested a “development path” of mark variograms: Large mature trees are more or less randomly distributed in the forest. They are surrounded by clusters of many small trees. Since there are many more small trees than large trees, the influence of the latter on the shape of the mark variogram is small. As time goes by, more and more of the small trees die or are removed by people. As a result the influence of large mature trees increases, i.e. pairs of large and small trees at short distances gain a larger weight. Thus the mark variogram has larger values for small r than for large r . Ford (1975) and Suzuki et al. (2008) refer to this phenomenon as local size hierarchy.

Reed and Burkhart (1985) suggested another development path for plantation forests: In young even-aged plantations positive autocorrelation prevails, i.e. the variogram shape is the one known from geostatistical variograms. As stands develop prior to self-thinning, spatial autocorrelation becomes negative as dominant

trees suppress neighbouring trees, i.e. a local size hierarchy develops. Self-thinning processes homogenise the plantations again, leading eventually to positive autocorrelation.

The literature review has demonstrated that mark variograms have been reported in several papers, and attempts have been made to explain the reasons for the appearance of unusual variograms. However, no systematic study of the possible shapes of such variograms and the underlying ecological and human influences – which lead to them – has been carried out.

In the present paper we provide a more detailed and systematic explanation of the mark variogram. We first give a definition and interpretation of the mark variogram and explain why its shape can differ from the shape of the geostatistical variogram. Then, the paper presents two additional data sets, based on long-term monitoring of forest development, where patterns leading to mark variograms with negative autocorrelation appear.

We complement the data analysis with modelling using a modified version of the individual-based model published in Pommerening et al. (2011a). Simulations allow us to study more systematically what the effects of different management and ecological processes are on marked point patterns of trees. The individual-based model is fitted separately to the two time series with nonlinear regression techniques implemented in R (R Development Core Team, 2012; Jones et al., 2009). We have selected the following four types of simulation-based analyses in order to explore the causes for different variogram shapes:

- (i) *Reconstruction of the original time series (forestry thinning)* by including forest management and growth-based natural mortality
- (ii) *Purely growth-based natural mortality*
- (iii) *Completely random tree removal*
- (iv) *Forestry thinning coupled with birth process* by reconstructing the original two case studies in (i) coupled with a natural regeneration of trees.

Items (ii)–(iv) were analysed in a normative way as examples to illustrate the consequences of alternative forest development types. In analogy to Yeong and Torquato (1998) these simulation-based analyses can also be interpreted as an inverse problem with the objective to find out under which ecological conditions negative autocorrelated mark variograms are realisable at all.

2. Materials and methods

2.1. Data sets

In this study, we deliberately concentrate on monospecies woodlands with constant environmental co-variables throughout the observation windows to focus the investigation on intraspecific tree interaction.

The short time series № 301 belongs to a replicated thinning experiment in naturally regenerated pure Norway spruce (*Picea abies* (L.) KARST.) at Karlstift (Austria, longitude: 14°45'59.7", latitude: 48°34'50.8"). In the research plot 31 (Table 4) the stem numbers were initially drastically reduced coupled with successive moderate thinnings. The plot has been surveyed three times spatially explicitly between 1994 and 2004.

The time series Embrach 41–194 (Table 5, longitude: 8°10'22.13", latitude: 47°22'18.32") belongs to a Swiss thinning trial in beech (*Fagus sylvatica* L.). The trees have been re-measured seven times between 1940 and 1991 including tree locations. As part of a frame-tree based thinning strategy there is a tendency to thin dominant trees before suppressed trees, which gives rise to a greater variation in tree size.

A more detailed data description can be found in Pommerening et al. (2011a). For preparing tree location maps in Tables 4 and 5 we used the Spatstat package (Baddeley and Turner, 2005).

2.2. Mark variograms

To study correlation between marks, the mark variogram can be used. It is defined as the conditional expectation of the mark difference (Eq. (1)) given that there is a point of the process located both at \mathbf{x} and at $\mathbf{x} + \mathbf{r}$, namely

$$\gamma_m(r) = \frac{1}{2}E(m(\mathbf{x}) - m(\mathbf{x} + \mathbf{r}))^2 = \frac{1}{2}E(m(o) - m(\mathbf{r}))^2; \quad r \geq 0. \quad (1)$$

Here, \mathbf{x} and $\mathbf{x} + \mathbf{r}$ denote the locations of two arbitrary points, o is the origin, \mathbf{r} is a difference vector of length r and $E(\cdot)$ is the expectation. Note that we assume stationarity and isotropy of the underlying marked point process which implies that $\gamma_m(r)$ only depends on the length r of the difference vector \mathbf{r} . With increasing r , the mark variogram approaches the variance of the mark (also called mark variance) σ^2 , which reflects the situation that the marks are stochastically independent. The mark variogram offers two interpretable characteristics (see Fig. 1), the correlation range, expressed by the distance r_{corr} , where $\gamma_m(r)$ is equal to σ^2 , and the interaction strength, $\gamma_m(0+)$, which is the upper limit of the mark variogram for very small values of r . Large values of r_{corr} indicate large correlation ranges. Furthermore, large values of $\gamma_m(0+)/\sigma^2$ express large size differences between points (i.e. tree locations) at close proximity, and are usually assumed to imply strong interaction (see Fig. 1, right). The mark variogram has small values if the marks of the points in a pair with interpoint distance r are similar and large values if the marks differ strongly. The mark variogram is typically estimated by an edge-corrected kernel estimator (see for example Illian et al., 2008, p. 354).

The definition of the mark variogram appears to be very similar to the definition of the geostatistical variogram, which is used to study the variability of regionalised variables taking values in the whole space (forest) and not only at some specific tree locations (see e.g. Cressie, 1993; Chilès and Delfiner, 1999; Wackernagel, 2003). It is defined as

$$\gamma_m(r) = \frac{1}{2}E(Z(\mathbf{x}) - Z(\mathbf{x} + \mathbf{r}))^2 = \frac{1}{2}E(Z(o) - Z(\mathbf{r}))^2; \quad r \geq 0, \quad (2)$$

where $Z(\mathbf{x})$ is the regionalised variable at location \mathbf{x} , also referred to as the random field. The random field is assumed to be stationary

and isotropic. The typical shape of geostatistical variograms is presented by the grey curve in Fig. 1 (left). The range of spatial correlation, r_{corr} , is the distance with $\gamma(r) = \sigma^2$ for $r \geq r_{\text{corr}}$. The nugget effect or nugget variance indicates short-range irregularities caused by very small structures or measurement errors.

Regionalised variables measured at short distances are similar, and therefore lead to typical geostatistical variograms, which increase with increasing distance. The mark variogram, however, is based on measurements at some specific (tree) locations and can, therefore, have different shapes. If there is no correlation between marks, the mark variogram is just a horizontal line, i.e. $\gamma_m(r)$ is constant. If trees of similar size are arranged in clusters, the mark variogram has a shape similar to a geostatistical variogram even though the marks are tree characteristics and not observations from a random field. García (2006) discussed the implications of such mark variograms for modelling. However, occasionally there are many close pairs of trees with one large tree and one small tree in a tree pattern leading to mark variograms with the shape of the black curve in Fig. 1. This shape is very different from the shape of a geostatistical variogram (see also Wälder and Stoyan, 1996; Stoyan and Wälder, 2000; Suzuki et al., 2008) reflecting negative autocorrelation with large size differences between neighbouring trees, i.e. large individuals are likely to be close to small ones and vice versa (Suzuki et al., 2008). In other words negative autocorrelation is an expression of high small-scaled diversity of tree sizes.

For simplicity and better understanding this paper concentrates on the case that there is no spatial correlation of a geostatistical nature, i.e. that the mark variogram only presents information on interaction and birth-and-death processes.

2.3. Individual-based model

Based on ideas of Adler (1996), Illian et al. (2008) and Berger and Hildenbrandt (2000) an individual-based model was developed by Pommerening et al. (2011a). In this model, a random field is constructed that describes a competition load structure resulting from additively superimposing competition impulses of single trees in a forest. The basic model equations can be found in Table 1 and the model parameters are listed in Table 2. The enumeration in Table 1 follows the enumeration in Pommerening et al. (2011a).

The annual diameter increment, $id_{i,t}$, (Eq. (A.3) in Table 1) for each tree i and time t is obtained as the product of potential diameter increment, $id_{i,t}^{\text{pot}}$, a growth parameter ν and the standardised competition load, $c_{i,t}^{\text{trans}}$. The potential diameter increment, $id_{i,t}^{\text{pot}}$ (Eq. (A.4)) is based on the first derivative of the Chapman-Richards growth function.

Every tree j emits a local competition impulse or signal at time t , which can be measured at any location ξ and depends on the tree's diameter, $dbh_{j,t}$, and the distance, $dist_j(\xi)$, between tree j and location ξ . The sum of the competition load of all trees at the location of tree i (Eq. (A.5) in Table 1) provides a measure of competition load of this tree. This competition load is then transformed to $c_{i,t}^{\text{trans}}$ (Eq. (A.6)) to involve the diameter of tree i and standardised so that the values are between 0 and 1.

For more plausibility Eq. (7) in Pommerening et al. (2011a) was modified to

$$md5_{i,t} = md_{i,t} \cdot md_{i,t-1} \dots md_{i,t-4}. \quad (3)$$

The diameter multiplier, $md5_{i,t}$, was then transformed to the diameter increment percentage of the last 5 years, $pd5_{i,t}$, following Wenk et al. (1990, p. 95):

$$pd5_{i,t} = 100\% \cdot \left(1 - \frac{1}{md5_{i,t}} \right). \quad (4)$$

Table 1

Sub-models of the individual-based model by Pommerening et al. (2011a) describing growth and competition processes. Enumeration of the formulae follows the enumeration in Pommerening et al. (2011a). Variable names are explained in Table 2.

Equation	Sub-model	Formula
(A.3)	Diameter increment	$id_{i,t} = id_{i,t}^{pot} \cdot v \cdot (1 - c_{i,t}^{trans})$
(A.4)	Potential diameter increment	$id_{i,t}^{pot} = Akp \exp(-k \cdot dbh_{i,t}) \cdot (1 - \exp(-k \cdot dbh_{i,t}))^{p-1}$
(A.5)	Competition load from shot-noise field	$c_{i,t} = \sum_{j \neq i} dbh_{j,t}^{\alpha} \exp\left(-\frac{\delta \cdot dist_{ij}(\xi_i)}{dbh_{j,t}^{\beta}}\right)$
(A.6)	Standardised competition load	$c_{i,t}^{trans} = \frac{c_{i,t}}{dbh_{i,t}^{\alpha} + c_{i,t}}$

During a period of 5 years past growth performance of trees is assessed. This method has been successfully used before in other mortality models (Berger and Hildenbrandt, 2000; Pommerening et al., 2011a). If the diameter increment percentage of the last 5 years is smaller than a prescribed critical value $pd5^{crit}$, the corresponding tree dies. For more details of this individual-based model and its theory, see Pommerening et al. (2011a).

A general problem with many long-term time series available from forestry experiments is that the cause of death has not been properly recorded. This is also the case in the two time series used in this study. Therefore we could not separate trees that died naturally from those that were cut in thinnings. However, we believe that separating these two causes of death in the model is crucial for understanding the influence of thinnings on autocorrelation patterns. We have solved this problem experimentally by reconstructing the original time series as per objective (i) in the introduction.

2.3.1. Reconstruction of the original time series (forestry thinning)

The documentation of the beech time series specifically states that a variant of frame-tree based thinning was applied (Leibundgut, 1966). Frame trees, usually between 80 and 200 trees per hectare, are selected and marked by foresters early in stand development and are then systematically promoted in every thinning by removing competing tree neighbours. A similar management regime can be assumed for the Norway spruce time series. Based on this information we developed a mechanistic approach in an attempt to reconstruct the thinning behaviour as well as possible. In preliminary experiments we detected that a frame-tree based thinning alone would not suffice. The observed variogram pattern can only be reconstructed successfully with a combination of frame-tree based thinning and random thinnings from below. The latter involves the random removal of small-diameter trees in between the frame trees and introduces a limited amount of stochasticity.

At the beginning of each simulation n_f frame trees are selected. First, all trees are sorted by diameter in descending order. Then the 1/3 largest trees are appointed as candidate frame trees. Now the number of candidate frame trees is reduced to n_f , the number of final frame trees, that form the most regular pattern among the largest trees of the forest. For this purpose each candidate frame tree, i , is marked by $\min(dist_{ij})$, the distance to the nearest candidate frame tree neighbour, j . Finally the frame tree candidate with the smaller stem diameter from the pair of trees with the smallest value of $\min(dist_{ij})$ is discarded and $\min(dist_{ij})$ is recomputed for the remaining frame tree candidates. This procedure is repeated until the specified number of final frame trees, n_f , is achieved. All other trees are referred to as matrix trees. This method guarantees a pattern of large-diameter frame trees that is as regular as possible which often is a silvicultural requirement.

Every year when a thinning is scheduled in the original time series up to n_c competitors of frame trees are removed. This is a dependent thinning of matrix trees given the frame trees. To identify frame tree competitors first the competition load, $c_{k,l}^{trans}$, is quantified (see Eq. (A.5) and (A.6) in Table 1) for each matrix tree k and each frame tree l . As a result each matrix tree is marked with a vector of dimension n_f . A matrix tree k is removed as part of the frame-tree based thinning if $c_{k,l}^{trans}$ is larger than a given threshold, c_{thresh} , and if $c_{k,l}^{trans}$ is among the n_c largest values for some frame tree l with $l = 1, \dots, n_f$. This thinning type was inspired by the way of constructing Matérn soft-core processes (Stoyan, 1987).

In addition to the frame-tree based thinning, a random thinning of small diameter trees is performed. The main role of the random thinning from below is to remove small-sized matrix trees, which are located outside the immediate neighbourhood of frame trees and therefore have almost no interaction with them. The removal of such trees increases the significance of pairs of trees consisting of a large frame tree and a small matrix tree at close proximity. This is also a dependent thinning given the frame trees. Every year a thinning is scheduled in the original time series, n_{thin} matrix trees are randomly removed. To ensure a thinning from below, the trees to

Table 2

Site and species-specific growth, competition and mortality parameters of the two spatial time series Embrach, Switzerland, Plot 41-194 (*Fagus sylvatica* L.) and Karlstift, Austria, Plot 31 (*Picea abies* (L.) KARST.).

Parameters	Description	Embrach	Karlstift
Av	Diameter increment parameter: product of parameter A in the potential diameter increment model (A.4) and parameter v in the diameter increment estimation (A.3).	45.5338	19.4911
k	Parameter in the potential diameter increment model (A.4).	0.0300	0.0790
p	Parameter in the potential diameter increment model (A.4).	4.0000	8.2574
α	Shot-noise parameter scaling impulse strength (A.5).	3.3372	0.9126
β	Shot-noise parameter scaling impulse range (A.5).	0.1744	0.6689
δ	Shot-noise parameter scaling impulse range (A.5).	1.1878	11.5286
$pd5^{crit}$	Mortality parameter (4).	0.0050	0.0500
T	Observation period of the research site in years.	51	10
$RMSE$	Root mean square error of annual diameter increment estimation in cm.	0.1016	0.1384
$Bias$	Bias of annual diameter increment estimation in cm.	-0.0005	0.0043

Table 3
Site and species-specific thinning and birth parameters of the two spatial time series Embrach, Switzerland, Plot 41–194 (*Fagus sylvatica* L.) and Karlstift, Austria, Plot 31 (*Picea abies* (L.) KARST.). Reco. – Reconstruction of the original time series (forestry thinning), Reco.+Birth – Forestry thinning coupled with birth process. The scenarios “purely growth based natural mortality” and “completely random tree removal” do not require parameters from this table.

Parameters	Description	Embrach		Karlstift	
		Reco.	Reco.+ Birth	Reco.	Reco.+ Birth
n_f	Number of frame trees.	21	21	18	18
n_c	Maximum number of frame tree competitors to be removed around each frame tree.	3	3	3	3
c_{thres}	Competition threshold for potential frame tree competitors.	0.015	0.015	0.010	0.010
n_{thin}	Relative frequency of trees available to be thinned.	0.75	0.75	0.45	0.45
d_{thin}	Upper threshold of the ratio dbh_i/d_g for thinned trees.	0.6	0.6	0.6	0.6
r_{thin}	Minimum distance (in metres) of thinned trees to frame trees.	2.4	2.4	3	3
b	Weibull scale parameter for birth process.	–	5	–	4
c	Weibull shape parameter for birth process.	–	5	–	5
n_{sap}	Number of tree saplings to be added to the point pattern.	–	500	–	750

be thinned need to have a ratio of tree diameter to quadratic mean diameter smaller than d_{thin} . In addition no thinned tree should be closer to any of the frame trees than r_{thin} .

2.3.2. Purely growth based natural mortality

For this development pathway, we assume that there is no man-made thinning of trees and that the most weakly growing trees die. For better comparison with the other three scenarios, in any year indicated as “thinning year” the same number of trees is removed by the model as in the original time series. Those trees have the lowest values of $pd5_{i,t}$ (see Eq. (3)). This type of tree mortality is purely deterministic.

2.3.3. Completely random tree removal

In this approach, the trees to be removed are selected at random in the years specified in the time series as thinning years. The numbers of trees to be thinned are again those given in the original time series. This thinning type acts as a theoretical control in this experiment and is, in contrast to the previous forest development path, purely stochastic.

2.3.4. Forestry thinning coupled with birth process

There are many different ways of modelling the establishment of new trees based on point processes, see for example Batista and Maguire (1998), Shimatani (2009) and Nanos et al. (2010). Here, we consider a method, which is both simple and realistic for the two species under consideration. Large numbers of tree saplings are assigned to locations according to a homogeneous Poisson process, i.e. new tree locations are uniformly distributed in the study region and are independent of each other. The birth process is assumed to coincide with the beginning of the time series and the initial diameters of the small trees are considered to be distributed according to a Weibull distribution. We would like to emphasise that the idea is not to find the most appropriate birth scenario but to see how newly arrived small trees affect the shape of the mark variogram. To compare different birth scenarios would be a subject for another paper.

The thinning parameters of simulation scenarios 2.2.1 and 2.2.4 can be found in Table 3. Note that the thinning parameters are needed only in the reconstruction of the original time series, not in the natural mortality and independent thinning scenarios.

2.4. Evaluation of simulation results

In order to be able to evaluate the simulation results properly, we felt that the distribution of marks (here the dbh or diameter distribution) was also a necessary summary characteristic in addition

to the mark variogram. This allowed us to check whether approximately the same number of trees and a similar size distribution was achieved as in the original time series. For this purpose we allocated all tree diameters to 4 cm-classes at the end of the observation period. Then we simply joined the numbers of trees in each class with lines. These simple graphs allowed us to check simultaneously the shape of the mark distributions and the number of trees.

To illustrate the goodness of fit of the different reconstructions mentioned above, we have plotted the empirical and model (simulation) based mark variogram and dbh distribution for each case. The simulation-based distributions are plotted together with 95% envelopes from each reconstruction. The envelopes are point-wise envelopes, where the values of the mark variogram (or dbh distribution) are sorted by each distance (or diameter class). The lower and upper envelopes give the 2.5% and 97.5% quantiles of the sorted values, respectively. The 95% envelopes are based on simulated replicates to assess the magnitude of variation. Naturally no envelopes exist in the case of purely growth-based simulation since mortality is purely deterministic.

3. Results

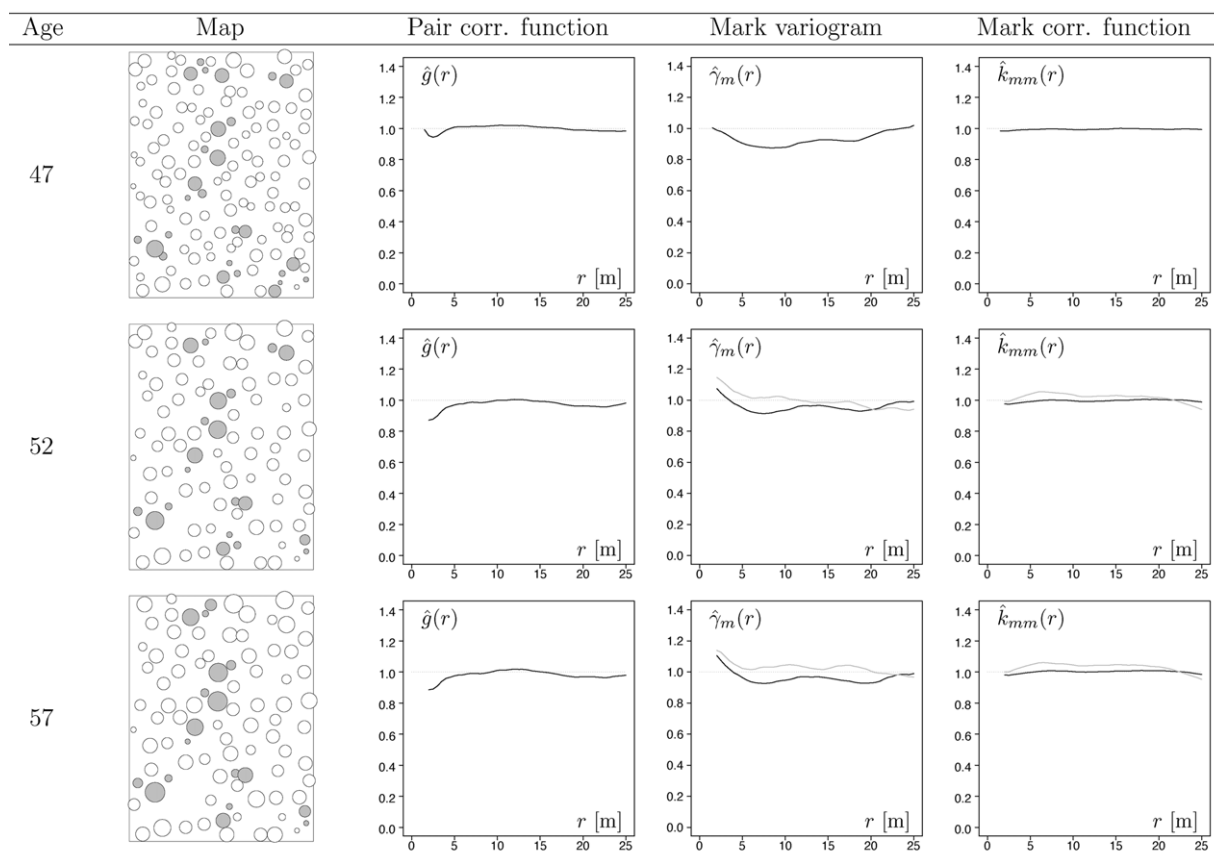
3.1. Analysis of the data sets

We plotted the pair correlation function, $g(r)$, the mark correlation function $k_{mm}(r)$, and the mark variogram, $\gamma_m(r)$, for both the Karlstift Norway spruce and the Embrach beech data. These functions and their estimation are described in detail in Illian et al. (2008). We have selected a comparatively large bandwidth, $h=4$, since in this study we focus on the overall trends, particularly at small distances, rather than on small details of the functions. Both diameter at breast height (dbh) and diameter increment were used as marks to see whether there are any fundamental differences in the resulting mark variograms. To ease the comparison between mark variograms estimated by using diameters and diameter increments as marks, we included the mark variance in a normalisation term.

In the Norway spruce data (Table 4) the negative autocorrelation of the marks at short distances (see $\gamma_m(r)$ and $k_{mm}(r)$) increased from 47 to 57 years of age as a result of some very limited thinning. The unusual shape of the mark variogram is thought to be a consequence of growth and competition processes, which increase particularly the dbh of dominating trees whilst dominated trees remain small. The effect of negative correlation, however, is not very strong. Using diameter increments as marks generally showed a stronger negative autocorrelative effect than using diameters at breast height, especially for small r . In contrast, the mark and pair

Table 4

Research plot 31 of the Austrian Norway spruce thinning experiment 301 at Karlstift (30 × 40 m). In the maps the trees are proportional to their diameters at breast height (*dbh*). The filled circles denote pairs of trees with the 20% largest values of $\frac{1}{2}(m(\mathbf{x}) - m(\mathbf{x} + \mathbf{r}))^2 r^{-2}$ that are chiefly responsible for the negative autocorrelation. The mark variograms were normalised with the mark variance. The dashed line in the mark variogram charts denotes the field variance or variance of marks. Furthermore, $\hat{g}(r)$ is the estimated pair and $\hat{k}_{mm}(r)$ is the estimated mark correlation function. Both tree diameters (black curve) and annual periodic diameter increments (grey curve) were used as marks with the mark variogram and the mark correlation function. A bandwidth $h = 4$ was used with the Epanechnikov kernel.



correlation functions did not vary much during the 10-year observation period.

In the Embrach beech data (Table 5), as time went by, the pair correlation function indicates increasing inhibition, i.e. competition in ecological terms, between plant locations as the trees became larger in diameter. The mark correlation function suggests that inhibition of marks markedly increased over time, particularly with diameter increment. The mark variograms changed drastically from a situation with a flat shape at the beginning, which indicates hardly any spatial correlation, to a strongly negatively autocorrelated mark variogram at 142 years of age. Again this effect was stronger for diameter increment than for tree diameters at short inter-tree distances, but the difference was small.

3.2. Simulation studies

All four reconstruction models, namely forestry thinning, natural mortality, random thinning and forestry thinning coupled with birth process, were fitted to the two data sets. In the preliminary analysis, we used both *dbh* and *dbh* increment as marks. However, the general trend as to the type of spatial correlation has always been the same with both variables. Therefore we decided to restrict the presentation of the results to tree diameters as marks and to the mark variogram as spatial summary characteristic, since the case $k_{mm}(r) > 1$ hardly occurs when tree diameters are used as marks, see Pommerening et al. (2011b).

The general trend of the Karlstift Norway spruce time series is well reproduced in the forestry thinning (see column 1, Table 6),

although the observed curves are not always inside the envelopes. Given the limited amount of stochasticity in this scenario we based the 95% envelopes on 20 simulation replications. The variation in the diameter distribution between distances 9 and 18 cm is caused by the different groups of small trees that were removed during the simulations of the thinning from below.

The mark variance based on natural mortality is markedly lower than the empirical mark variance, and the mark variogram is almost constant throughout the distance range (see column 2, Table 6). The simulated diameter distribution reveals that there are no trees smaller than 15 cm *dbh* followed by a surplus of large trees between 25 and 35 cm at the end of the observation period.

The third scenario, completely random tree removal or independent thinning, was simulated with 100 replications, since there is more variability than in the natural mortality due to the purely stochastic nature of mortality. The observed mark variogram being inside the envelopes is more an indication of the large variability than a good fit of the model (column 3, Table 6). The simulated diameter distribution indicates a surplus of trees between 28 and 42 cm *dbh*.

The last scenario combines the reconstruction of the first column with a birth process (column 4, Table 6). Again, the envelopes are based on 100 replications. The mark variance is also larger here than in the original time series. The diameter distributions of the simulations are similar to that of the original time series, except that according to this approach the number of trees is larger around 8 cm *dbh* compared to the original time series.

Table 5
 Research plot 41-194 of the Swiss beech thinning experiment at Embrach (51 × 49 m). In the maps the trees are proportional to their diameters at breast height (*dbh*). The filled circles denote pairs of trees with the 20% largest values of $\frac{1}{2}(m(\mathbf{x}) - m(\mathbf{x} + \mathbf{r}))^2 r^{-2}$ that are chiefly responsible for the negative autocorrelation. The mark variograms were normalised with the mark variance. The dashed line in the mark variogram charts denotes the field variance or variance of marks. Furthermore, $\hat{g}(r)$ is the estimated pair and $\hat{k}_{mm}(r)$ is the estimated mark correlation function. Both tree diameters (black curve) and annual periodic diameter increments (grey curve) were used as marks with the mark variogram and the mark correlation function. A bandwidth $h = 4$ was used with the Epanechnikov kernel.

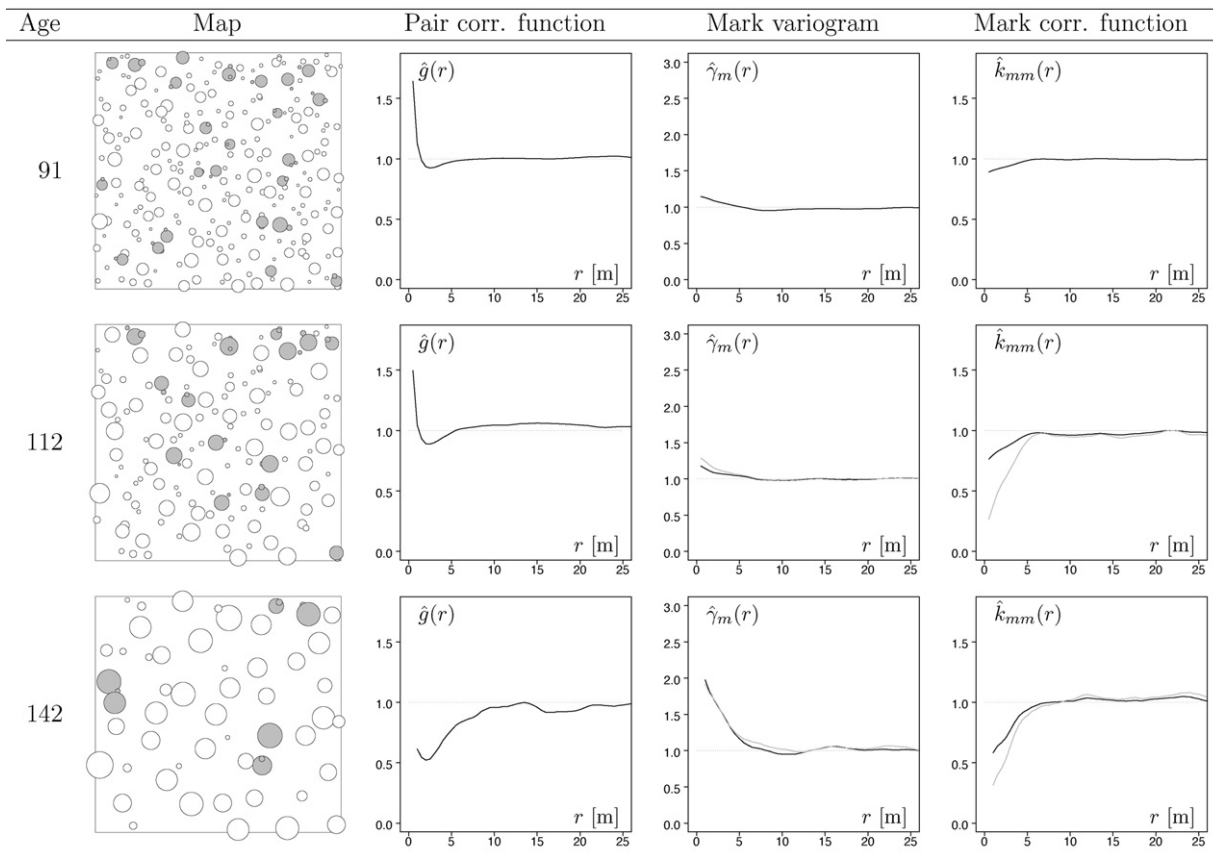


Table 6
 Mark variograms and diameter distributions of the Austrian Norway spruce research plot 31 at the end of the observation period in 2004 obtained from the four simulation scenarios detailed in Section 2. The black continuous lines represent the original time series. The dotted lines give the 95% envelopes. The dashed lines indicate the mark variance.

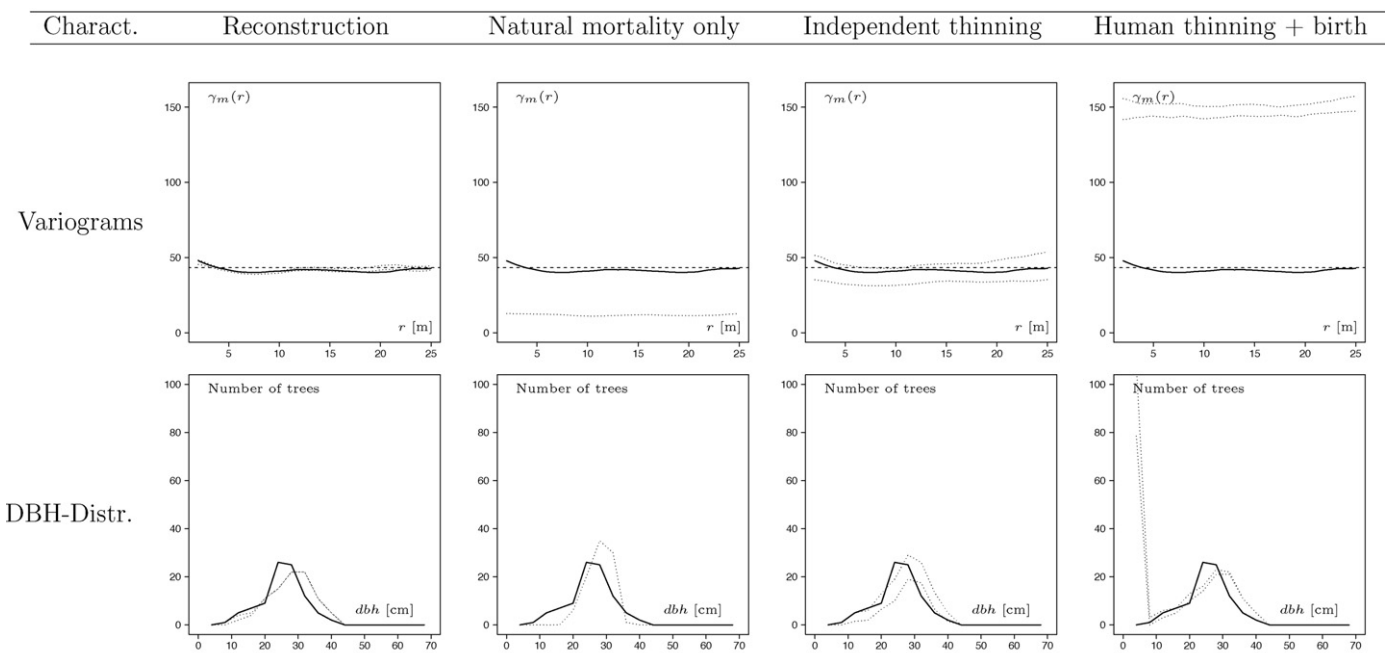


Table 7

Mark variograms and diameter distributions of the Swiss beech research plot 41-194 at the end of the observation period in 1991 obtained from the four simulation scenarios detailed in Section 2. The black continuous lines represent the original time series. The dotted lines give the 95% envelopes. The dashed lines indicate the mark variance.

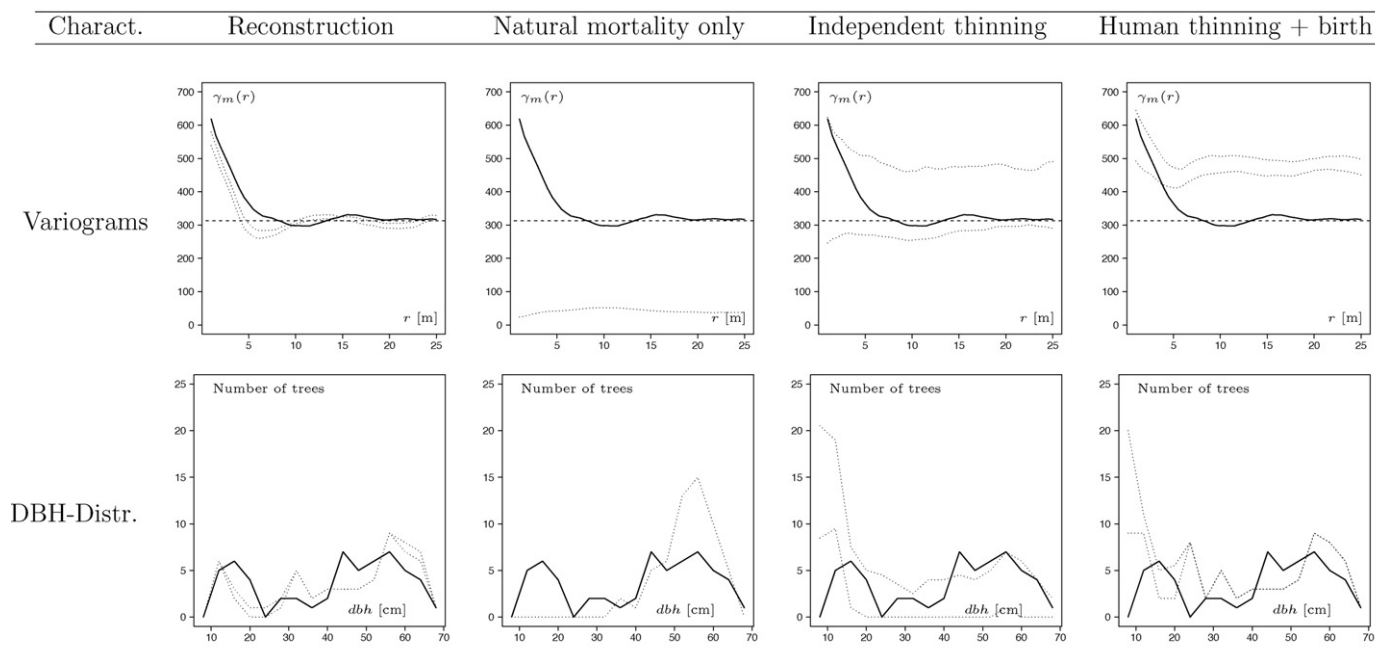


Table 7 gives the results for the Embrach beech time series. Again, the general trend of the time series was well reproduced in the forestry thinning simulation (column 1). The diameter distribution shows that there is some stochasticity in the ranges between 15 and 30 cm and between 59 and 65 cm due to the choice of small trees that were removed.

The purely growth-based natural mortality scenario (column 2, Table 7) led to a markedly lower mark variance compared to that of the original time series and the mark variogram values are again almost constant throughout the distance range. The simulated diameter distribution suggests that there are no trees smaller than 30 cm dbh but a surplus of large trees between 50 and 70 cm at the end of the observation period.

The results of the independent thinning show that the observed mark variogram is again mostly inside the envelopes, since variation is rather large (column 3, Table 7). The simulated diameter distribution exhibits a considerable surplus of small trees up to 15 cm and of large trees between 40 and 55 cm.

The results of the combined scenario “human thinning+birth” highlight a much larger mark variance than without the birth process (column 4, Table 7). The envelopes also show that the shape of the mark variogram is similar to that of the original time series, i.e. it also indicates negative autocorrelation. The simulated diameter distributions are somewhat similar to those resulting from independent thinning with slightly more medium and large sized trees. In both cases the number of small trees is much larger than observed in the original data, since either not enough small trees were removed in the independent thinning or too many small regeneration trees survived.

In all simulation scenarios the correlation range did not differ much from the one in the two original time series.

4. Discussion

We have demonstrated that the mark variogram is a useful tool when studying correlation between the sizes of trees at close proximity. Furthermore, we have explained that the shape of the mark variogram can be very different from the shape of the geostatistical

variogram since the mark variogram is based on tree characteristics, not on regionalised variables. The main purpose of this paper was to find reasons for the unusual shape caused by negative autocorrelation, i.e. that neighbouring trees tend to be of different sizes. We were able to show that man-made thinning is an important factor causing negative autocorrelation.

The preliminary analysis of the two datasets shows that negative autocorrelation variograms appear typically in some limited time periods in the development of a forest. Such time periods are often characterised by strong interactions between neighbouring trees that cause size hierarchies. The case studies also show that using dynamic tree attributes as marks such as diameter increments can lead to a stronger effect than the use of static variables such as diameters or heights.

In our study, we simulated the two tree time series, Karlstift Norway spruce and Embrach beech, by using the individual-based model developed by Pommerening et al. (2011a) combined with four different thinning methods, forestry thinning, natural mortality, random thinning and forestry thinning coupled with birth process. The underlying individual-based growth and interaction processes as determined by the model parameters and structure have been the same in each thinning simulation. However, the way the trees were either removed (natural mortality, thinning) or added (birth process) to the marked point pattern differed between the scenarios.

First, we studied the scenario, where the medium-sized competitors of frame trees were removed as well as some of the small trees between the frame trees. As expected, this very specific type of man-made tree removal resulted in mark variograms indicating negative autocorrelation. The mark variograms obtained were very similar to those observed in the original time series, i.e. the mark variograms indicated negative autocorrelation as a result of deliberate human management aiming at reducing the competition pressure on certain desired trees.

Our second and third simulation scenarios were based on natural mortality and on random tree removal (independent thinning), respectively. Neither of them led to negative autocorrelation indicating that negative autocorrelation is not necessarily a typical

behaviour in naturally growing forests and neither is a product of pure chance. In certain very specific circumstances and by considering other marks than the diameter, such as in the study by Suzuki et al. (2008), one may find negative autocorrelation between marks developing in natural forests without human disturbances.

With our last scenario combining human thinnings with birth processes we were able to show another pathway to negative autocorrelation. This, however, only works if the number of pairs of large and small trees at close proximity is statistically balanced (see Section 2.2.1). Similarly to the study by Suzuki et al. (2008), excessive numbers of small regeneration trees were subsequently removed by natural mortality and thinning. As a result the mark variance was much larger than in the original time series.

5. Conclusions

Taking the literature (Reed and Burkhart, 1985; Biondi et al., 1994; Kint et al., 2003; Dimov et al., 2005; Suzuki et al., 2008) and our own experiments into consideration we can conclude that we have identified five processes causing negative autocorrelation in mark variograms:

1. Natural self-thinning during the stem exclusion phase (Oliver and Larson, 1996),
2. Selective forestry thinnings promoting size differentiation,
3. Selective forestry thinnings/harvesting promoting birth processes,
4. Natural competition processes leading to a differentiation of tree sizes (understorey reinitiation and old growth stages according to Oliver and Larson, 1996),
5. Natural/human disturbances leading to the retention of a few old large trees which gives rise to mass colonisation by small trees followed by self-thinning among the small trees (understorey reinitiation and old growth stages according to Oliver and Larson, 1996).

Our study particularly highlighted cause 5, i.e. that disturbances, either natural or man-made or a combination of both, are major causes of patterns with negative autocorrelation. They lead to a removal (death) of trees, and later to an increase of small trees followed by death of some of the small trees. Therefore, they can induce the development of local size hierarchies and negative autocorrelation and create temporary situations of high size diversity. Birth processes increase the mark variance and are the most important processes leading to negative autocorrelation which is a temporary expression of high small-scaled diversity of tree sizes. Beyond this point in time some of the smaller trees are out-competed and die and others approach the size of their larger neighbours. Sometimes also new waves of incoming small regeneration trees destroy the pattern of negative autocorrelation.

We have shown that negatively autocorrelated mark variograms are linked to disturbances. Therefore, this summary characteristic is indeed an important tool in the analysis of disturbance ecology.

Acknowledgements

The authors thank Dietrich Stoyan for supporting this study with valuable advice. Annett Degenhardt (Eberswalde Forestry State Centre of Excellence, Eberswalde, Germany) and Pavel Grabarnik (Russian Academy of Sciences, Pushchino, Russia) sent helpful comments on an earlier draft of this paper. Andreas Zingg (Swiss Federal Institute for Forest, Snow and Landscape Research WSL, Birmensdorf, Switzerland) has kindly provided the *Embrach* time series data. Markus Neumann (Austrian Federal Research and Training Centre

for Forests, Natural Hazards and Landscape, Vienna, Austria) contributed the *Karlstift* time series data to this study for which the authors are very grateful. Aila Särkkä was financially supported by the Swedish Research Council and the Swedish Foundation for Strategic Research. She would also like to thank the Department of Statistics at the University of Washington for its hospitality during the time this paper was completed. Helpful comments of two anonymous reviewers are gratefully acknowledged.

References

- Adler, F.R., 1996. A model of self-thinning through local competition. *Proceedings of the National Academy of Science of the United States of America* 93, 9980–9984.
- Baddeley, A., Turner, R., 2005. *Spatstat: An R package for analyzing spatial point patterns*. *Journal of Statistical Software* 12, 1–42.
- Batista, J.L.F., Maguire, D.A., 1998. Modeling the spatial structure of tropical forests. *Forest Ecology and Management* 110, 293–314.
- Berger, U., Hildenbrandt, H., 2000. A new approach to spatially explicit modelling of forest dynamics: spacing, ageing and neighbourhood competition of mangrove trees. *Ecological Modelling* 132, 287–302.
- Biondi, F., Myers, D.E., Avery, C.C., 1994. Geostatistically modeling stem size and increment in an old-growth forest. *Canadian Journal of Forest Research* 24, 1354–1368.
- Chilès, J.-P., Delfiner, P., 1999. *Geostatistics. Modeling Spatial Uncertainty*. John Wiley & Sons, New York, pp. 695–699.
- Cressie, N., 1993. *Statistics for Spatial Data*. Revised edition. John Wiley & Sons, New York, pp. 900–909.
- Dimov, L.D., Chamber, J.L., Lockhart, B.R., 2005. Spatial continuity of tree attributes in bottomland hardwood forests in the southeastern United States. *Forest Science* 51, 532–540.
- Ford, E.D., 1975. Competition and stand structure in some even-aged plant monocultures. *Journal of Ecology* 63, 311–333.
- García, O., 2006. Scale and spatial structure effects on tree size distributions: implications for growth and yield modelling. *Canadian Journal of Forest Research* 36, 2983–2993.
- Illian, J., Penttinen, A., Stoyan, H., Stoyan, D., 2008. *Statistical Analysis and Modelling of Spatial Point Patterns*. John Wiley & Sons, Chichester, pp. 534–539.
- Jones, O., Maillardet, R., Robinson, A., 2009. *Introduction to Scientific Programming and Simulation Using R*. Taylor & Francis Ltd, Boca Raton, 453 pp.
- Kint, V., van Meirvenne, M., Nachergale, L., Geudens, G., Lust, N., 2003. Spatial methods for quantifying forest stand development: a comparison between nearest neighbor indices and variogram analysis. *Forest Science* 49, 36–49.
- Leibundgut, H., 1966. *Die Waldpflege (Forest management)*. Verlag Paul Haupt, Bern, 192 pp.
- Nanos, N., Larson, K., Millerón, M., Sjöstedt-de Luna, S., 2010. Inverse modelling for effective dispersal: do we need tree size to estimate fecundity? *Ecological Modelling* 221, 2415–2424.
- Oliver, C.D., Larson, B.C., 1996. *Forest Stand Dynamics*. Update edition. John Wiley & Sons, New York, USA, 520 pp.
- Pommerening, A., LeMay, V., Stoyan, D., 2011a. Model-based analysis of the influence of ecological processes on forest point pattern formation—a case study. *Ecological Modelling* 222, 666–678.
- Pommerening, A., Gonçalves, A.C., Rodríguez-Soalleiro, R., 2011b. Species mingling and diameter differentiation as second-order characteristics. *Allg. Forst- u. J.-Ztg.* 182, 115–129.
- R Development Core Team, 2012. *R: A language and environment for statistical computing*. R Foundation for Statistical Computing, Vienna: <http://www.R-project.org>
- Reed, D.D., Burkhart, H.E., 1985. Spatial autocorrelation of individual tree characteristics in loblolly pine stands. *Forest Science* 31, 575–587.
- Shimatani, I.K., 2009. Spatially explicit neutral models for population genetics and community ecology: Extensions of the Neyman-Scott clustering process. *Theoretical Population Biology* 77, 32–41.
- Stoyan, D., 1987. Statistical analysis of spatial point processes: a soft-core model and cross-correlations of marks. *Biometrical Journal* 29, 971–980.
- Stoyan, D., Wälder, O., 2000. On variograms in point process statistics, II: Models of markings and ecological interpretation. *Biometrical Journal* 42, 171–187.
- Suzuki, S.N., Kachi, N., Suzuki, J.-I., 2008. Development of a local size-hierarchy causes regular spacing of trees in an even-aged *Abies* forest: analyses using spatial autocorrelation and the mark correlation function. *Annals of Botany* 102, 435–441.
- Wackernagel, H., 2003. *Multivariate Geostatistics. An Introduction with Applications*. Springer Verlag, Heidelberg, pp. 387–389.
- Wälder, O., Stoyan, D., 1996. On variograms in point process statistics. *Biometrical Journal* 38, 895–905.
- Wenk, G., Antanaitis, V., Šmelko, Š., 1990. *Waldertragslehre*. [Forest yield science.] Deutscher Landwirtschaftsverlag, Berlin, 448 pp.
- Yeong, C.L.Y., Torquato, S., 1998. Reconstructing random media. *Physical Review E* 57, 495–506.